# Finite Difference Time Domain Analysis of Photonic Crystal Resonators

# تحليل رنانات البلورات الفوتونية باستخدام طريقة الفروق المحدودة في النطاق الزمني

**Nihal F. Areed, Salah S. A. Obayya. and Hamdi A. El-Mikati**

Department of Electronics and Electrical Communications Engineering, Mansoura University, Mansoura, Egypt.

**الملخص**: في هذا البحث تستخدم طريقة الفروق المحدودة في النطاق الزمني لتحليل انتشار النبضات المستقطبة كهربيا و عرضيا في مرشدات الموجات البصرية ذات التكوين البلوري و ذات انحناء 90°. و تتم مقارنة النتائج بطريقة انتشار الشعاع و المبنية على طريقة العناصر المحدودة لحساب معاملات الانتشار. و أوضحت المقارنة تطابق نتائج الطريقتين رغم أن الطريقة المقترحة يمكن تنفيذها بإمكانيات حاسب محدودة مقارنة بالطريقة الأخرى. و تم بعد ذلك دراسة تفصيلية للرنانات الحلقية المربعة ذات التكوين البلوري و تم دراسة الأبعاد التي تحقق النقل التام للموجات من إحدى قناتي الرنانة (Through channel) إلى القناة الأخرى(Drop channel) عند طول موجي ($\lambda$=1.55255 μm).

**Abstract:** A Finite Difference Time Domain (FDTD) analysis has been effectively applied to investigate the transmission of the transverse electric polarized pulses in 90° bend optical waveguide. Comparison with a Time Domain Beam Propagation Method (BPM) based on finite element scheme has been made and excellent agreement is achieved. Moreover, a detailed study of photonic crystal square ring waveguide resonator has been carried out. A series of simulations are performed to determine by how much the radius of holes would have to be tuned to result in radiation at $\lambda$ = 1.55255 μm (the center of the telecommunications c band) to be dropped.

*Index Terms*: photonic crystal, Finite Difference Time Domain Method (FDTD) , optical waveguide resonator.

## I. Introduction

A photonic crystal (PC) is a periodic arrangement of dielectric or metallic materials, and is an optical analogy to a conventional crystal. A conventional crystal can provide an energy band gap to prevent an electron from propagating through the crystal. A photonic crystal provides a possibility to control and manipulate the propagation of light. If, for some frequency range, no light of any polarization can propagate in a photonic crystal, the crystal is said to have a complete photonic band gap (PBG). If one introduces a line defect into a photonic crystal which has a photonic band gap, one can guide light (whose frequencies are within the photonic band gap) from one location to another since the light has nowhere else to go[1,2].

Resonant filters are attractive candidates for channel dropping, since they can potentially be used to select a single channel with a very narrow line width. Channel dropping filters, which can access one channel of a wavelength division multiplexed (WDM) signal while leaving other channels undisturbed, are essential[3].

Researches over the last decade have generated a wide range of rigorous numerical algorithms for modeling optical waveguide structures, such as plane-wave expansion (PWE) [4-5], and finite element methods [6]. These versatile algorithms have been applied with success to study issues such as transmissions and reflections for Photonic Crystal (PC) waveguides. In this paper, Finite Difference Time Domain (FDTD) Technique [7] has been utilized to analyze the Propagation properties of PC waveguide structures.

The paper is organized as follows. Following this introduction, a brief mathematical treatment of FDTD method is given in section II. The results and their physical explanation are detailed in section III. Finally, some conclusions are presented in section IV.

## II. Formulation

### A- Basic Equations

In a two-dimensional case, the fields can be decoupled into two transversely polarized modes, namely the E polarization ($E_z$, $H_x$, and $H_y$) and the H polarization ($H_z$, $E_x$, and $E_y$). Yee's

Accepted August 8, 2006

mesh is widely used in the FDTD analysis [7]. Here, Yee's two dimensional mesh in Finite Difference Time Domain solver is used. The unit Yee cell of the two-dimensional mesh for E polarization case is illustrated in Fig.1.

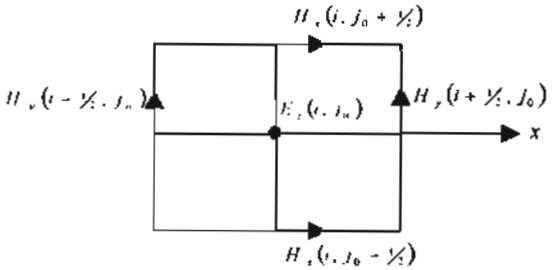


Fig. 1. The unit Yee cell of the two-dimensional FDTD mesh for E polarization case[7].

The continuity conditions are automatically satisfied since, all the transverse field components are tangential to the unit cell boundaries. The following 2-D FDTD time stepping formulas constitute the discretization (in space and time) of Maxwell's equations on a discrete two-dimensional mesh in a cartesian $x$ $y$ coordinate system for E polarization case:

$$H_x\left[i,j\right]^{n+\frac{1}{2}} = H_x\left[i,j\right]^{n-\frac{1}{2}} - \frac{\Delta t}{\mu_{i,j}}\left[\frac{E_z\left[i,j+1\right]^n - E_z\left[i,j\right]^n}{\Delta y}\right], \quad (1\text{-a})$$

$$H_y\left[i,j\right]^{n+\frac{1}{2}} = H_y\left[i,j\right]^{n-\frac{1}{2}} + \frac{\Delta t}{\mu_{i,j}}\left[\frac{E_z\left[i+1,j\right]^n - E_z\left[i,j\right]^n}{\Delta x}\right], \quad (1\text{-b})$$

$$E_z\left[i,j\right]^{n+1} = \frac{\varepsilon_{i,j} - \sigma_{i,j}\Delta t/2}{\varepsilon_{i,j} + \sigma_{i,j}\Delta t/2} E_z\left[i,j\right]^n + \frac{\Delta t}{\varepsilon_{i,j} + \sigma_{i,j}\Delta t/2}\left[\frac{H_y\left[i,j\right]^{n+1/2} - H_y\left[i-1,j\right]^{n+1/2}}{\Delta x} - \frac{H_x\left[i,j\right]^{n+1/2} - H_x\left[i,j-1\right]^{n+1/2}}{\Delta y}\right], \quad (1\text{-c})$$

and for H polarization case :

$$E_x\left[i,j\right]^{n+1} = \frac{\varepsilon_{i,j} - \sigma_{i,j}\Delta t/2}{\varepsilon_{i,j} + \sigma_{i,j}\Delta t/2} E_x\left[i,j\right]^n + \frac{\Delta t}{\varepsilon_{i,j} + \sigma_{i,j}\Delta t/2}\left[\frac{H_z\left[i,j\right]^{n+1/2} - H_z\left[i,j-1\right]^{n+1/2}}{\Delta y}\right], \quad (2\text{-a})$$

$$E_y\left[i,j\right]^{n+1} = \frac{\varepsilon_{i,j} - \sigma_{i,j}\Delta t/2}{\varepsilon_{i,j} + \sigma_{i,j}\Delta t/2} E_y\left[i,j\right]^n - \frac{\Delta t}{\varepsilon_{i,j} + \sigma_{i,j}\Delta t/2}\left[\frac{H_z\left[i,j\right]^{n+1/2} - H_z\left[i-1,j\right]^{n+1/2}}{\Delta x}\right], \quad (2\text{-b})$$

$$H_z\left[i,j\right]^{n+1/2} = H_z\left[i,j\right]^{n-1/2} - \frac{\Delta t}{\mu_{i,j}}\left[\frac{E_y\left[i+1,j\right]^n - E_y\left[i,j\right]^n}{\Delta x} - \frac{E_x\left[i,j+1\right]^n - E_x\left[i,j\right]^n}{\Delta y}\right] \quad (2\text{-c})$$

where the superscript $n$ indicates the discrete time step, the subscripts $i$ and $j$ indicate the position of a grid point in the $x$, and $y$ directions, respectively. $\Delta t$ is the time increment, and $\Delta x$, and $\Delta y$ are the space increments between two neighboring grid points along the x and y directions, respectively. $\omega$ is the angular frequency, $\mu$ , $\varepsilon$ and $\sigma$ are the permeability, the permtivity and the conductivity of the medium considered.

### B- Boundary Conditions

When calculating the band structures of photonic crystals, one naturally chooses a unit cell of lattice as the finite computation domain, and uses the periodic boundary condition, which satisfies the Bloch theory [2]. Therefore, we have the following simple boundary conditions for updating the fields,

$$\begin{aligned} \overline{E}(\overline{r} + \overline{L}) &= e^{i\beta L}\,\overline{E}(\overline{r}), \\ \overline{H}(\overline{r} + \overline{L}) &= e^{i\beta L}\,\overline{H}(\overline{r}). \end{aligned} \quad (3)$$

where L is the lattice vector.

A perfectly matched layers (PML) with the following impedance matching condition [8] is applied to bound the computational window. In the PML, the electric or magnetic field components are split into two subcomponents (e.g., $E_z = E_{zx} + E_{zy}$) with the possibility of assigning losses to the individual split field components.

$$\frac{\sigma_e}{\varepsilon_o n^2} = \frac{\sigma_m}{\mu_o} \quad (4)$$

where $\sigma_e$ and $\sigma_m$ are the electric and magnetic conductivities of the PML, respectively, and $n$ is the refractive index of the adjacent computing domain. which means that the wave impedance of a PML medium exactly equals to that of the adjacent medium in the computing window regardless of the angle of propagation.

### C- Stability Condition

For two-dimensional FDTD time-stepping formulas, the stability conditions for orthogonal case is [7]

$$\Delta t \le 1 \Big/ \left[c\sqrt{\Delta x^{-2} + \Delta y^{-2}}\right] \quad (5)$$

### D- Frequency Transformation

With the FDTD method, all the fields are obtained in the time domain. However, the dispersion relation (the band structures, guided modes, etc) of a photonic crystal is a relation between the frequency and the wave vector. Therefore, we need to perform a Fourier transform. MATLAB package ver.7 is adopted to evaluate this transform and evaluate the phase shift constant β.

## III. Numerical results

First, we used the 2-D FDTD numerical method outlined above to calculate the transmitted and reflected power spectra around a 90° sharp bend whose schematic diagram is shown in Fig.2-a [9]. Figure 2-b shows the input TE mode pulse with a central wavelength 1.55μm which is located in the transverse y direction at the reference point *P1*. The time variation of the field is recorded at the reference points *P2* and *P3*, respectively as shown in Fig.3. This structure has been discretized with a uniform mesh where the computational window sizes [ x × y ] are [ 30μm × 30μm ], the time step $\Delta t$ is 0.023586 *fs* and the simulation time is 800 *fs*. The PML layers are assumed to be 50 layers. On a PC (Pantium IV, 3.2GHz, 2GB RAM), the whole simulation period took around one hour and 25 min. The frequency dependence of the transmitted and reflected power spectra are shown in Fig.4. The results of the finite-element based time domain beam propagation method [9] are also shown on the same figure. Comparison between the results of the two methods shows a satisfactory agreement. However, the FDTD method is simpler and was effectively carried out on the Pantium IV PC .

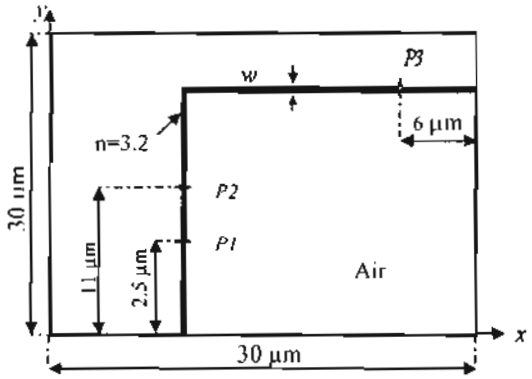


(a)

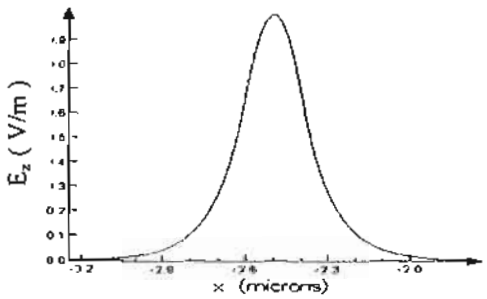


(b)

Fig. 2. A 90° sharp bend (a) Details of the structure $w$ = 0.2 μm, (b) Input TE mode pulse at point *P1*.

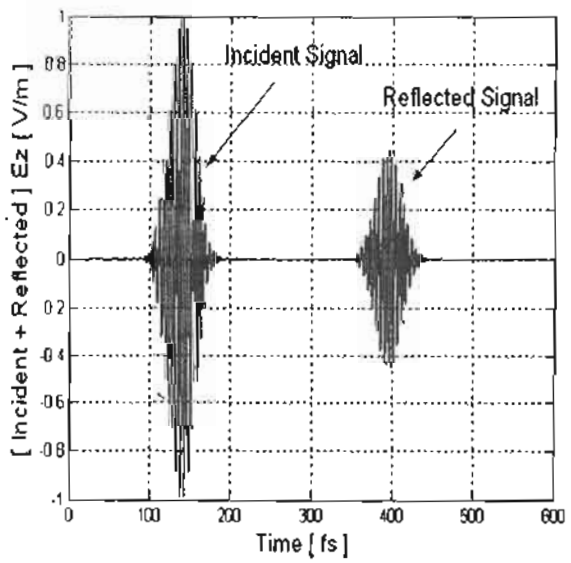


(a)

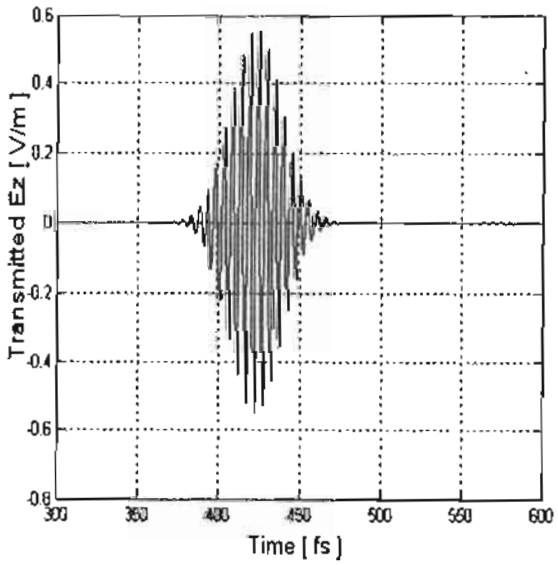


(b)

Fig.3. Time variation of the field recorded at points: (a) *P2*, (b) *P3*.

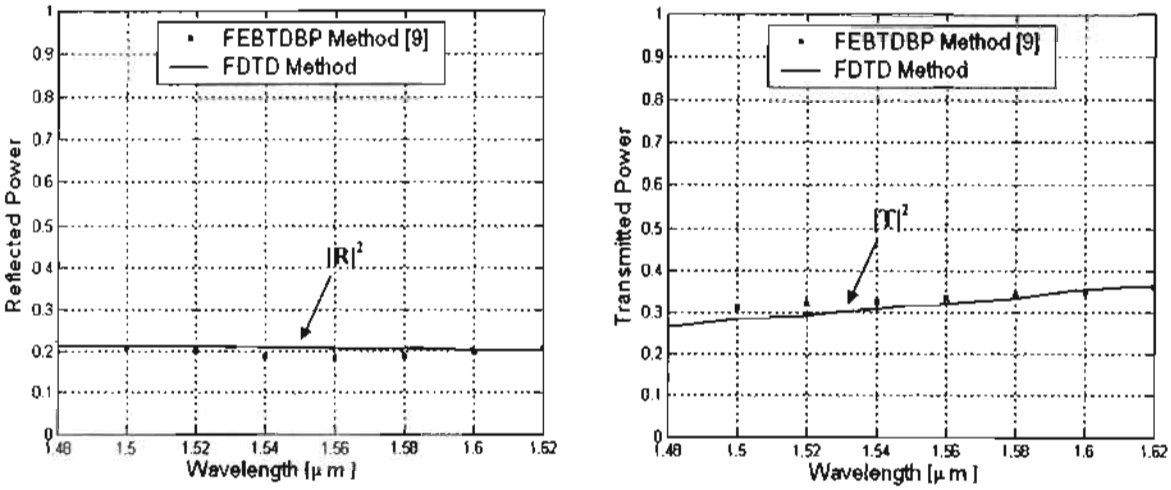


Fig. 4. Power spectra around a 90° sharp bend (a) Reflected $|R|^2$, (b) Transmitted $|T|^2$.

Next, we consider a photonic crystal structure of dielectric rods arranged in air on a square array with a lattice constant $A$ as shown Fig.5.a [10,11]. Figure 5-b shows the calculated band structure of the cosidered square lattice in TE mode. From the figure one can see that, the crystal has a PBG for TE modes which extends from $\lambda = A/.302\mu m$ to $\lambda = A/.443$ μm. Figure 6-a shows a 90° bend with an element division in the neighboorhood of the corner[10]. This structure has been discretized with a uniform mesh where the computational window sizes [ x × y ] are [ 51.6019μm × 51.6019μm ], the time step $\Delta t$ is 0.0641259 *fs* and the whole simulation time is 350 *fs*. The PML is assumed to have a thickness of 3.5μm. One gaussian pulse with $\lambda_o$ = 1.45 μm is sent down the waveguide covering different ranges of frequencies. On the same used PC, the whole simulation period took around 2 hours and 25 min. The reflection and transmission charcterstics calculated at port 1 and port 2, respectively are shown in the Fig. 6-a. Figure 6-b shows the electric field patterns of the pulse with gaussian profiel propgating in the cosidered 90° bend waveguide, the figure demonstrates that the transmission is a little deteriorated. The results obtained using the presented 2-D FDTD are in very good agreement up to realibility of figure in these references [10,11].

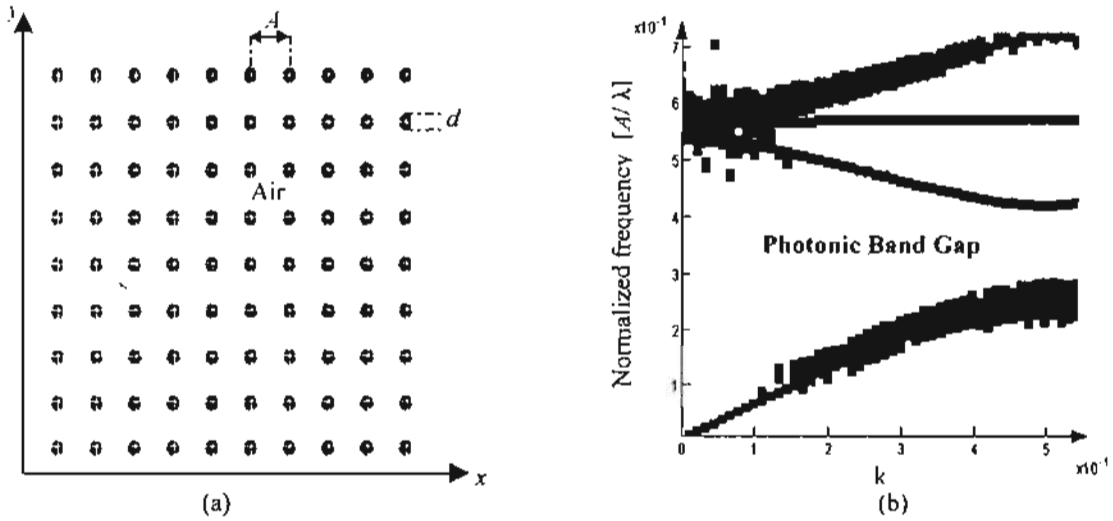


Fig. 5. Cross section of square lattice of dielectric rods arranged in air: (a) Details of the structure $A$ = 0.58 μm, $d$=.36$A$, $n$=3.4, (b) Calculated band structure for TE mode.

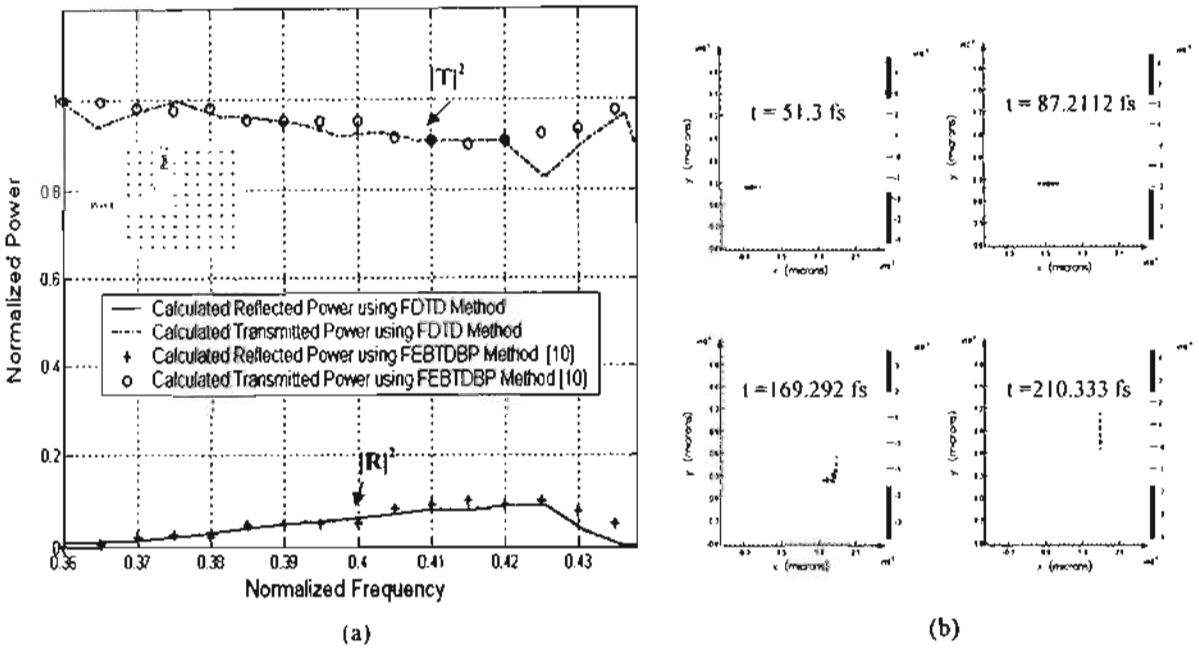


Fig. 6. A 90° bend photonic crystal waveguide: (a) Propagation characteristics , (b) Snapshots of the propagating pulse at different time periods.

Next, we consider the mode supported by the photonic crystal waveguide at the center of the telecommunication band 193.1 THz. The waveguide itself is formed by removing one line of dielectric rods of the square lattice shown in Fig.5.a. as observed in Fig.7.a. To keep reasonable accuracy, this structure has been discretized with a uniform mesh where the computational cell steps [ $\Delta x \times \Delta y$ ] are [ 0.0261μm × 0.0261μm ], the time step $\Delta t$ is 0.0307805 *fs* and the whole simulation time is 2500 *fs*. The whole simulation period took around 7 hours and 17 min. Figure 7.b shows the excitation gaussian pulse with $\lambda_0$ = 1.55 μm. The time domain electric field signal, monitored for sufficiently long time at point *P2* is shown in Fig.8.a. As may be observed from this figure, this time monitor ensure that the radiation has for the most part, left the simulation volume. Also, in order to find the mode of interest, the data collected by the frequency domain monitor at 193.1THz found at point *P2* is used as shown in the inset of Fig.8.b.

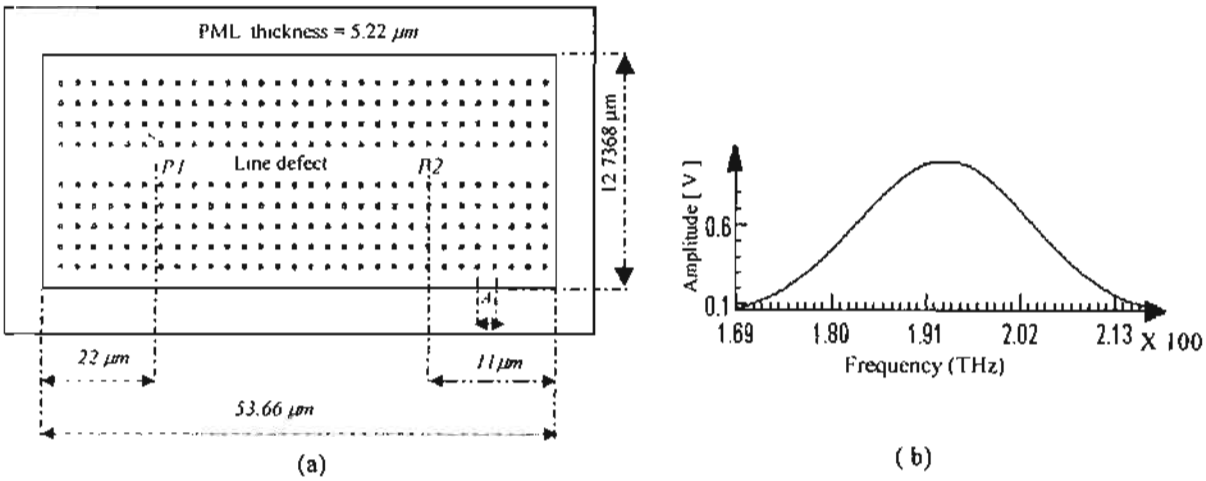


Fig. 7. Photonic crystal waveguide of dielectric rods in air : (a) Details of the structure $A$ = 0.58 μm, $d$=.36$A$, $n$=3.4, (b) Input Gaussian pulse at *P1*.

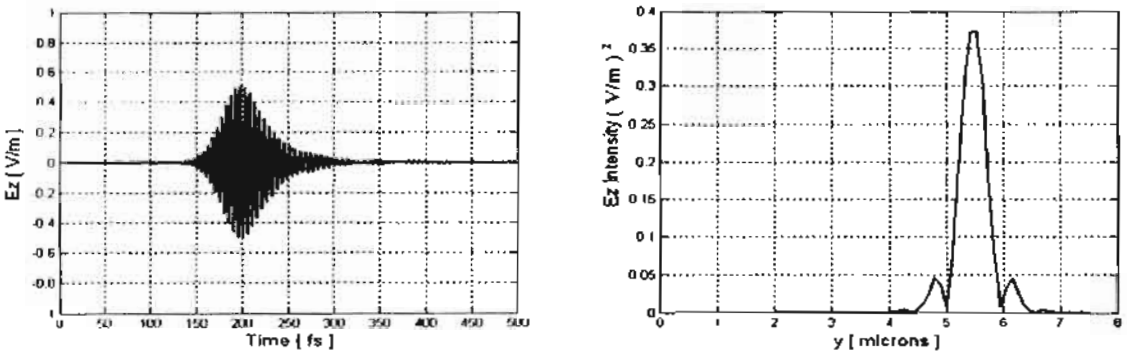


(a) (b)

Fig. 8. Photonic crystal waveguide of dielectric rods in air: (a) Time domain signal at *P2*, (b) Calculated TE mode at $\lambda = 1.55$ μm.

Finally, we consider the light transmission through an optical ring resonator. This structure consists of two line defects (a "through" channel, and a "drop" channel) connected by a square ring defect of dimensions *a* and *b* as shown in Fig.9.a. The waveguides comprising the drop and through channels and the ring resonator consist of a core that is 0.9512 μm wide and has refractive index 1. This structure has been analyzed using the same computational window of the above analyzed photonic crystal waveguide. The calculated TE mode pulse shown in Fig.8.b with a central wavelength 1.55 μm is used for the excitation of the through channel and is located in the transverse x direction at point *P1*. Figure 9.b monitors the time signal in the drop waveguide. As may be observed, this signal contains seven pulses, which correspond to seven round-trips of the ring. Figure 10.a shows the steady-state field profiles at 193.1THz for different values of *a* and *b*. As may be noted from the figure, the interested frequency is approximately dropped at dimension $a = b$; where, The magnitude of the normalize power transmission with respect to the input source power for the square ring case at 193.1 THz is about 0.61 as shown in Fig.10.b.

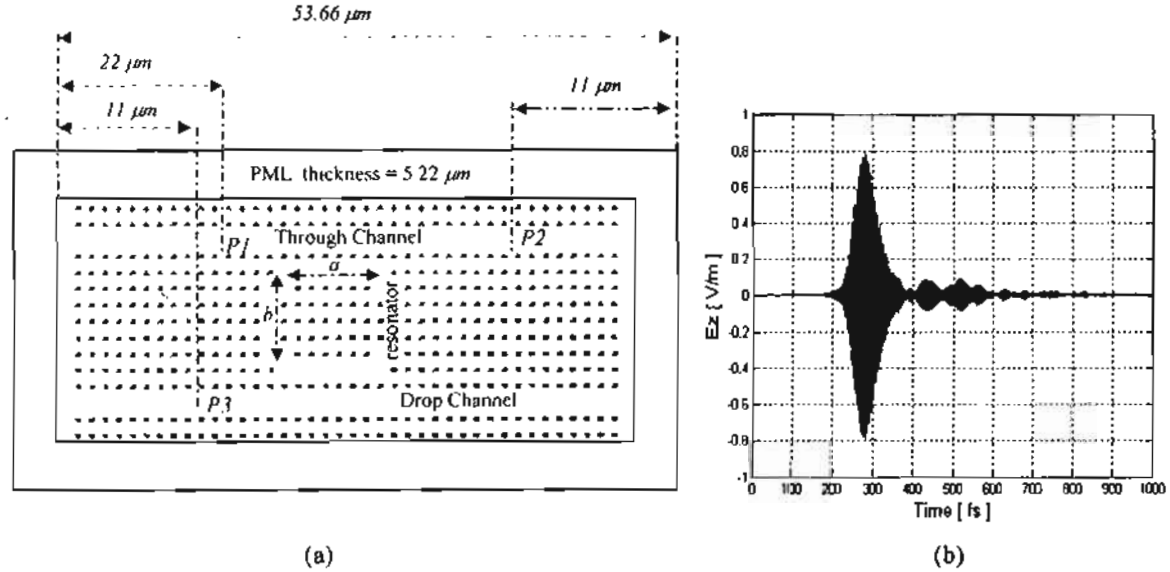


(a) (b)

Fig. 9. photonic crystal Ring Resonator of dielectric rods in air: (a) Details of the structure, (b) A time variation of the field recorded at points at *P3*

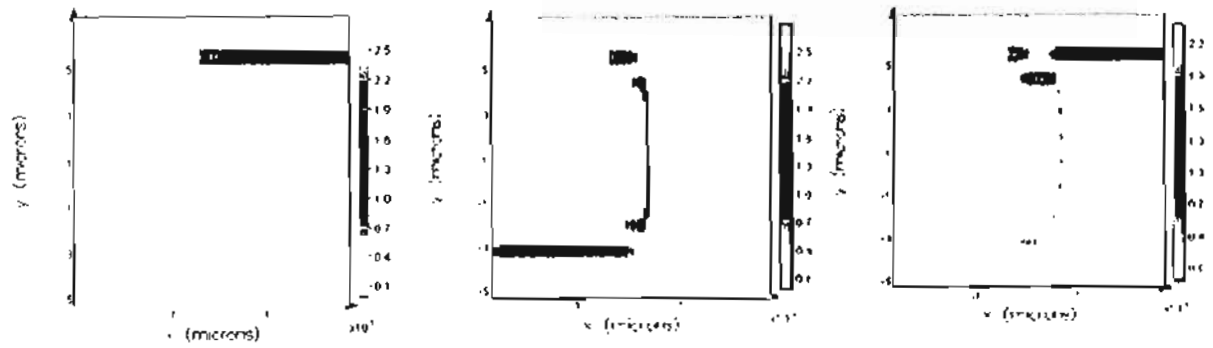


(a)

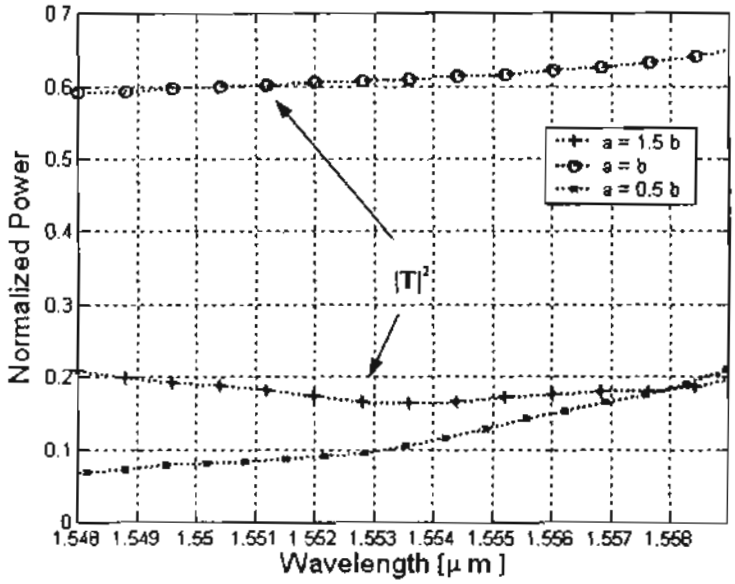


(b)

Fig. 10. photonic crystal Ring Resonator of dielectric rods in air : (a) steady state field profile at $\lambda$ = 1.55μm for: Case 1: $a$=0.5 x $b$, $b$ = 5.8$\mu m$, Case 2: $a$ = $b$ = 5.8$\mu m$ and Case 3: $a$ = 1.5x $b$, $b$ =5.8 $\mu m$, (b) The transmitted power to the drop channel.

Therefore, these encouraging results have stimulated further efforts seeking better performance. In this respect, the proper choice of the radius of the holes on the inner edges of the square ring resonator would be possible to optimize the performance of the transmission. To this end we run a series of simulations to determine the optimum hole radius and the whole simulation period took around 72 hours. Figure 11.a shows the fractional transmission as a function of hole radius, and demonstrates that the radius of the holes would have to be modulated from the original 0.1044 μm to 0.09135 μm to efficiently divert a signal at 193.1THz from the through channel to the drop channel as observed from the calculated steady state profile shown in Fig.11.b. Figure.11.c shows the magnitude of the transmitted normalized power to the through and the drop channels for the optimum case.

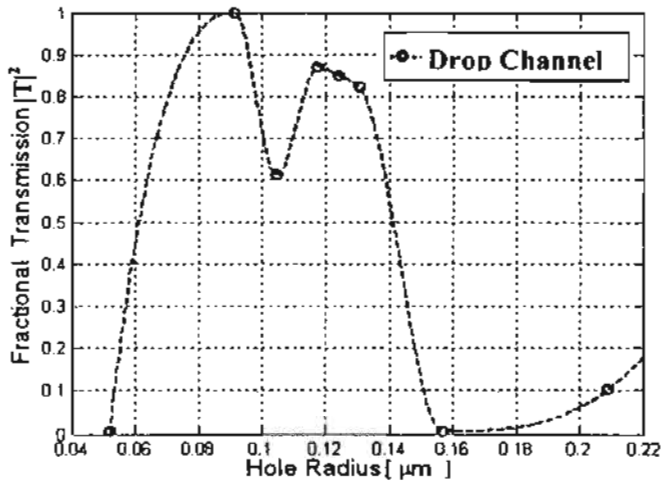


(a)

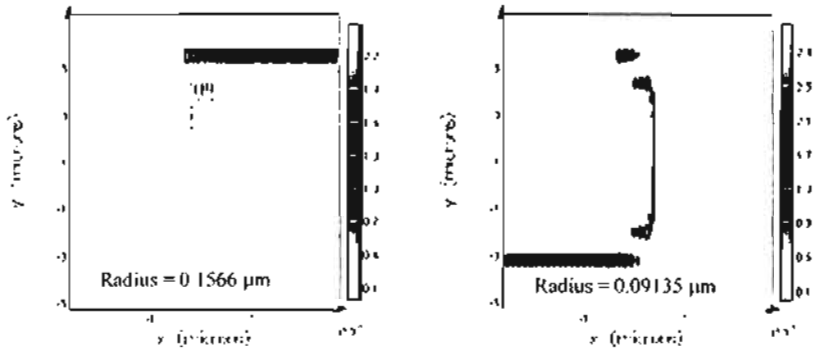


(b)

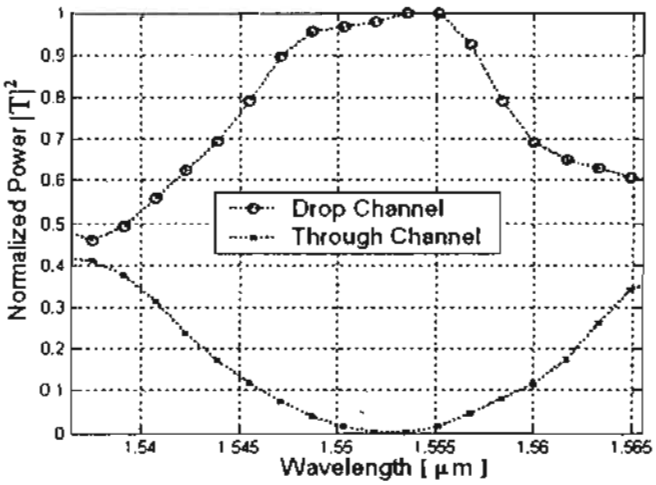


(c)

Fig. 11. Simulation of Ring Resonator: (a) Fractional transmission vs. Hole radius, (b) Steady state field profile at $\lambda$ =1.55 μm for different Hole radii, (c) The propagation charctersitics at hole radius = 0.09135 μm.

## IV. Conclusion

Finite difference Time Domain algorithm incorporated with Bloch periodic or perfectly matched layer absorbing boundary condition is formulated for the analysis of 90° sharp bend waveguide and 90° curved bend PC waveguide. Moreover, an efficient series of simulation developed to efficiently transmit the a signal at 193.1THz from the through channel to the drop channel in the suggested optical square ring resonator which is designed in a square lattice of dielectric rods arranged in air. This designed structure is useful in optical communication integerated circuits.

## V. References and Links


1. Min Qiu, Computational methods for the analysis and design of Photonic bandgap structures, Ph. D., Royal Institute of Technology, Stockholm, 2000.

2. Joen I. Kim , Analysis and applications of microstructure and holey optical fibers, Ph. D., Virginia State University, 10 Sept. 2003.

3. *http://abinitio.mit.edu/photons/index.html*,

4. Ferrando, E. Silvestre, J. J. Miret, P. Andres and M. V. Andres, "Full-vector analysis of a realistic photonic crystal fiber," Opt. Lett. 24, pp. 276-278 (1999).

5. S. G. Johnson and J. D. Joannopoulos, "Block-iterative frequency-domain methods for Maxwell's equations in a planewave basis," Opt. Express 8, pp. 173-190 (2001),

   *http://www.opticsexpress.org/abstract.cfin?URI=OPEX-8-3-173*

6. F. Brechet, J. Marcou, D. Pagnoux, and P. Roy, "Complete analysis of the characteristics of propagation into photonic crystal fibers by the finite element method," Opt. Fiber Technol. 6, pp. 181-191 (2000).

7. *http://www.ee.udel.edu/~dprather/classes/eleg840/lectnotes/lect10.ppt*

8. Chin-Ping Yu and Hung-Chun Chang, "Yee-mesh-based finite difference eigenmode solver with PML absorbing boundary conditions for optical waveguides and photonic crystal fibers," Opt. Express, Vol. 12, No. 25, pp. 6165-6177, 13 December 2004.

9. S. S. A. Obayya, "Efficient Finite Element Based Time Domain Beam Propagation Analysis of Optical Integrated Circuits," IEEE Journal of Quantum Electronics, Vol. 40, No. 5, pp. 591-595, May 2004.

10. Masanori Koshiba, Yasuhide Tsuji, Masafumi Hikari, "Time Domain Beam Propagation Method and Its Application to Photonic Crystal Circuits," IEEE Journal of Lightwave Technol., Vol. 18, No. 1, pp. 102-110, January 2000.

11. Jasmin Smajic, Christian Hafner, Daniel Erni, "Design and optimization of an achromatic photonic crystal bend," Opt. Express, Vol. 11, No. 12, pp. 1378-1384, 16 June (2003).